Diversification dynamics of the Palaeozoic actinopterygian radiation

Joseph T. Flannery-Sutherland[1*], Struan Henderson[1], Sophie A. Fasey[1], Sam Giles[1]

[1]School of Geography, Earth and Environmental Science, University of Birmingham, Birmingham, UK; [*]Corresponding author. Emails: j.t.flannerysutherland@bham.ac.uk

Ray-finned fish are the most speciose vertebrate group today, but the dynamics of their early diversification are contentious. Their fossil record suggests a first radiation in the Carboniferous following the End-Devonian Mass Extinction events. Conversely, recent phylogenetic hypotheses imply a radiation originating in the Late Devonian, but lack the taxonomic breadth required to robustly test this. This necessitates phylogeny-free inference of actinopterygian diversification rates from fossil occurrences, itself challenging due to uncertain taxonomies, incomplete occurrence databases, and severe spatiotemporal sampling biases. Here, we analyse a revised dataset of all known Palaeozoic actinopterygian genera and species using approaches that accommodate spatial and temporal sampling variation. We detect elevated actinopterygian diversification in the Late Devonian, with substantially greater lineage survival across the Hangenberg extinction event than indicated by the fossil record. Surprisingly, we detect no positive shifts in origination across the event, refuting previous hypotheses of explosive actinopterygian radiation in its wake. Cryptic lineage diversification is reflected by increased diversity across different geographic scales in the Carboniferous, although this is overwhelmingly driven by low palaeolatitude Euramerican fossil assemblages. Instances where local and global actinopterygian diversity patterns are decoupled highlight the geographic heterogeneity of their Palaeozoic radiation, providing focus for future research efforts.

Keywords: fossil sampling bias; spatial standardisation; birth-death process; speciation; extinction; origination

1. Introduction

The explosive Carboniferous diversification of ray-finned fish (Actinopterygii) is generally considered to represent an adaptive radiation following the end-Devonian mass extinction events [1-3]. In their earliest history, after diverging from lobe-finned fish (Sarcopterygii) in the Silurian [4] and in sharp contrast to their sister clade, actinopterygians persisted at low diversity and ecological prominence for nearly 50 million years, represented by just a handful of undisputed occurrences through the Early and Middle Devonian, alongside fragmentary scale-based taxa with contested taxonomic affinities [5,6]. The Hangenberg extinction at the end of the Devonian marks a turning point where vertebrate faunas previously dominated by placoderms and sarcopterygians were rapidly supplanted by a more contemporary fauna composed of chondrichthyans and taxonomically and morphologically diversified actinopterygians [1-3,7-9].

Previous studies have posited that the Hangenberg event was directly responsible for the striking shifts in multiple facets of actinopterygian biodiversity [1,14,15]. This pattern appears borne out by phylogenetic hypotheses, which infer a bare minimum number of lineages to have survived the mass extinction event and bring the origin of the actinopterygian crown group in line with the Devonian-Carboniferous boundary [10-13]. However, a recent report of a Devonian actinopterygian deeply nested within an otherwise Carboniferous clade [12] raises an alternative scenario: that cryptic actinopterygian lineage diversification began in the Devonian, under markedly different ecological conditions, with much higher lineage survivorship across the Hangenberg event than previously thought. [12,15]. In turn, this suggests that radically different evolutionary mechanisms may have been responsible for the rise of actinopterygians. Although an intriguing possibility, the limited taxonomic scope of most existing phylogenetic studies makes it difficult to test whether the early Carboniferous radiation was fuelled by the explosive diversification of a few lineages following the Hangenberg event, or by the survival of a wider range of lineages which diverged during the Devonian [12]. Previous work has also typically recovered extensive polytomies between early actinopterygian taxa, and candidates for Devonian lineages seeding subsequent diversification in the Carboniferous, as well as relationships between Palaeozoic lineages and the actinopterygian crown, are unclear [11,16-21]. Consequently, incomplete trees and uncertain tree shapes present an ongoing hurdle for resolving the tempo and mode of the first radiation of actinopterygians.

In the absence of well resolved, taxonomically comprehensive phylogenies, our understanding the roots of actinopterygian success in the Carboniferous and through the Palaeozoic is reliant on a direct reading of their fossil record. Inference of their diversification dynamics based on fossil occurrences has proven challenging due to a lack of databases suitable for interrogating diversity trends, severe sampling biases in their fossil record, and historically problematic taxonomy [2,8,9,16]. Recent efforts have begun to address the lack of high-quality fossil occurrence databases of early actinopterygians but continue to highlight the other issues that plague their fossil record [8,9]. Further, patterns of relative diversity are useful indicators of the macroevolutionary success of a clade, but they are generally uninformative of the rates of origination and extinction responsible for changing diversity. A range of mechanisms may drive variation in these rates [22], with fundamentally different ecological implications for the processes which shaped early actinopterygian diversity. Interclade competitive exclusion by other gnathostomes would be characterised by suppression of origination, while environmental vulnerability would manifest in high extinction, but these rates have not yet been quantified. Both diversity and diversification processes are also vulnerable to spatial variation in the distribution and extent of the fossil record, yet these have not been investigated in actinopterygians using spatially sensitive frameworks which can both mitigate this major source of bias and reveal geographic variation in diversification dynamics [23-28]. Consequently, it is unknown whether the sharp increase in apparent actinopterygian diversity in the early Carboniferous might represent an artefact of spatial sampling bias in the fossil record, or if any increases in their geographic extent genuinely reflect their evolutionary radiation at this time.

Two broad strategies have been proposed to overcome spatial sampling biases, one better suited to estimating diversity, the other to estimating diversification rates. The first advocates for estimation of diversity from local subsamples of the fossil record where spatial sampling variation can be adequately controlled [23-25] and informative average trends drawn from this set of a reliable local estimates. The other approach favours the use of regional, spatially standardised datasets which capture taxon stratigraphic durations rather than just pointwise samples of diversity [26-27,29]. Origination and extinction rates can then be robustly estimated from these datasets using birth-death-sampling models which treat their set of taxa as forming a phylogenetically coherent subsample of a clade's true diversity, but without the requirement for a formal phylogenetic tree to inform the analysis [30-33]. In this paper, we investigate patterns of diversity and diversification rates in early actinopterygians using an

expanded fossil occurrence database coupled with these complementary analytical strategies to elucidate their rise to prominence through the Palaeozoic. We characterise diversification dynamics through the Palaeozoic to understand the extent to which the actinopterygian fossil record is biologically informative versus driven by sampling bias and focus on whether exceptional diversification dynamics were responsible for their early Carboniferous radiation.

2. Materials and methods

2.1 Fossil occurrence data. We assembled a revised occurrence dataset of all valid early actinopterygian genera and species, with substage level dating. This comprises 2142 Palaeozoic genus level actinopterygian occurrences of which 1644 (76.8%) are additionally classified to species level, across 907 collections with a mean collection age uncertainty of 4.1 Ma (median 2.8 Ma), plus 212 Early Triassic occurrences across 62 collections to minimise edge effects in our focal study window. Rather than using arbitrary equal length intervals or formal chronostratigraphic divisions in our downstream diversity analyses, we used the formation binning approach of Dean et al. [34] to optimise the temporal binning of our occurrence data according to its stratigraphic resolution. Full details on the assembly, cleaning and binning of our dataset are available in the supplementary information.

2.2 Spatial diversity patterns. We applied several different spatial subsampling schemes to our temporally binned occurrence data. These schemes cover a range of spatial resolutions, allowing us to deconvolve global actinopterygian diversification trends into their constituent geographic components, but also control biological signal versus sampling noise in different ways in our downstream analyses.

Our broadest schemes minimise fluctuations in the minimum spanning tree (MST) length of the global extent of the actinopterygian dataset through time using the method of Flannery-Sutherland et al. [26]. This approach yields display high taxonomic inclusion, making it suitable for investigating their phylogenetic diversification signal. We also investigated diversity trends in high, medium and low absolute palaeolatitude subsamples to investigate how their diversification may have varied spatially. As these datasets are still broad, they display highly uneven abundance distributions arising from aggregation of often taxonomically problematic occurrence data. Our final subsampling schemes address this issue, by using temporally binned data at the level of individual collections, and within equal

area grid cells to provide more reliable samples of local diversity from which average trends through time can be calculated.

We estimated genus diversity through time from each of our spatially subsampled datasets using sampled-in-bin diversity (SIB), range-through-time diversity (RTT), coverage-based rarefaction (CBR), and extrapolation by Squares (SQR). The former two metrics do not correct for uneven sampling between time bins, unlike the latter two, but still provide useful indications of the sampling structure and quality of the early actinopterygian fossil record. We favoured genus diversity in this instance as it is generally considered to be more robust to variation in sampling and taxonomic practice [35], although it is not a true substitute for species level diversity [36]. Full details on the methods and choices made during spatial subsampling, and the implementation of our diversity estimations, are available in the supplementary information.

2.3 Birth-death models. Diversity estimation in a spatially sensitive framework is useful for investigating geographic variation in actinopterygian richness, while avoiding many of the pitfalls of their fossil record. Diversity estimates themselves, however, are not necessarily informative about their underlying speciation and extinction rates, while geographically restricted estimates may not reflect the diversification dynamics responsible for total Palaeozoic actinopterygian phylogenetic diversity. Consequently, we inferred genus and species-level origination and extinction rates from our MST-standardised datasets to elucidate these dynamics whilst still controlling for the confounding effects of spatially biased sampling.

Traditional methods for inferring diversification rates from RTT and SIB data (e.g., second-for-third or three-timer rate metrics [37,38]) are often unreliable when confronted by clade fossil records which display low preservation rates and high turnover [39]. Instead, estimation methods which treat fossil occurrence data as the product of a birth-death-sampling process are more reliable [39]. We employ two such methods, chosen due to their complementary sets of model assumptions: a hierarchical birth-death-sampling model [30-32] and the skyline Fossilised Birth-Death Range model [33,40] hereafter referred to by their respective implementations in the software packages PyRate [31] and RevBayes [41]. Briefly, the key differential assumptions are variable versus constant sampling rates through time, and complete versus incomplete sampling of all fossil lineages that ever existed. Both PyRate and RevBayes ultimately produce the same set of results (estimates of origination, extinction, and

sampling rates through time), permitting direct comparison between their different model assumptions. Full details of the assumptions, implementations and parameters for all diversification rate analyses are available in the supplementary information.

3. Results

3.1 Spatiotemporal sampling of Palaeozoic actinopterygians. Bin-wise counts of actinopterygian occurrences are low through the Devonian until an increase in abundance in the Tournaisian stage of the Mississippian epoch of the Carboniferous (Fig. 1A). Further spikes occur late in the Visean stage of the Mississippian, through the Bashkirian stage of the Pennsylvanian epoch of the Carboniferous, and early in the Asselian and Wuchiapingian stages of the Early and Late Permian respectively, producing a saw-toothed sampling pattern through the Palaeozoic (Fig. 1A). There is little correspondence between spikes in occurrence counts and spikes in the spatial extent of the actinopterygian fossil record (Fig. 1B), with extents in the Devonian comparable to extents throughout the Carboniferous and Permian, despite counts in the latter greatly exceeding those in the former. Subsampling by MST length resulted in relatively minor loss of occurrences from the dataset but was generally effective in reducing fluctuations in spatial extent from the Serpukhovian stage of the Mississippian onwards (Fig. 1B). Standardised spatial extent fluctuates through the Devonian to the Visean, after which most bins fall within ±10% of our target, aside for a slight deficit early in the Bashkirian, and in the Changhsingian stage of the Late Permian where spatial extent slightly exceeds the target (Fig. 1B). Spatial extent falls well below our target spatial extent, however, in the Early and Middle Devonian and in the Mississippian, where there is a notable crash through the Visean (Fig. 1B).

Despite occurrence exclusion, MST standardisation has little effect on SIB and RTT genus diversity patterns from the Devonian to the Carboniferous, aside from moderate reductions in the Frasnian stage of the Late Devonian and in the Tournaisian (Fig 1C–1D). Sawtooth trends in SIB diversity are smoothed to some degree when RTT diversity is examined (Fig. 1D). RTT diversity accrued very slowly through the Devonian but increased by around an order of magnitude across the Devonian-Carboniferous boundary. Some diversity loss occurred into the early Visean before a second peak at the beginning of the Pennsylvanian, followed by decline through the remainder of the Carboniferous, then a

general trend of rising diversity through the Early Permian. This trend terminated with a drop in diversity in the Middle Permian, followed by a final spike in Changhsingian. The only instances where a crash in spatial extent following MST standardisation is accompanied by a clear drop in RTT diversity are in the early Visean and in the Moscovian stage of the Pennsylvanian. Otherwise, sampling of raw diversity appears to be decoupled from residual fluctuations in spatial extent (Figs. 1C–1D). Global trends in SIB genus diversity generally track with genus diversity estimated by CBR (Pearson correlation coefficient = 0.62, $p < 0.0001$) and SQR (Pearson correlation coefficient = 0.87, $p < 0.0001$) with little change between the total, windowed and MST-standardised datasets (Figs. 1E–1F). The major exceptions to this correspondence between raw and sampling-corrected diversity trends, however, are the patterns of relative richness in the Early Permian versus the rest of the dataset where CBR and SQR estimates in the former are heavily inflated compared to the latter (Figs. 1E–1F).

3.2 Actinopterygian diversity across spatial scales. SIB, RTT, CBR and SQR diversity at low palaeolatitudes from the Devonian to the early Bashkirian (Figs. 2A, 2D, 2G, 2J) recover similar trends those from the total dataset. RTT diversity then declined from the early Bashkirian peak in contrast to the total dataset, returned to early Carboniferous levels through the Early Permian, then rose again through the Middle to Late Permian. This is largely mirrored by SQR diversity, while CBR diversity instead peaked in the late Visean, before declining more gradually through the rest of the Carboniferous (Figs. 2G, 2J). Diversity trends in the mid and high latitudinal bands diverge from the low latitude signal and are more sensitive to the choice of diversity metric. Mid latitude RTT diversity (Fig. 2E) rose modestly in the Tournaisian, declined to Devonian levels in the early Visean, then increased sixfold through the Early Permian. This spike is recovered by CBR and SQR diversity, matching the anomalous spike observed in the total dataset from these metrics (Figs. 2H, 3K). Diversity at high latitude is sporadically sampled, varies between metrics, and cannot be interpreted with clarity (Figs. 2C, 2F, 2I, 2L).

Average collection diversity is generally similar between SIB, CBR and SQR metrics, but median diversity is frequently biased downwards by the prevalence of singleton actinopterygian collections (Fig. S1). Instead, we focus here on the results obtained from equal area grid cells. There is a distinct shift from low diversity to a high diversity regime across the Devonian-Carboniferous boundary, followed by small fluctuations through the

Mississippian, a more distinct drop in the late Pennsylvanian, a transient spike at the beginning of the Early Permian, then a broad pattern of stepwise increases to SIB diversity peak in the Guadalupian (Fig. 3A–3C). The signal from the total dataset is largely replicated when only grid cells from low palaeolatitudes are considered (Figs. 3D–3F). Mid latitude diversity is sporadically sampled through the Devonian and Carboniferous. Sampling in the Permian is more frequent, but diversity fluctuates between time bins without any clear trends (Figs. 3G–3I). While high latitude trends are more consistent between metrics, sampling is too sporadic to permit confident interpretation of any trends (Figs. 3J–3L).

3.3 Diversification rates. Actinopterygian genus and species origination (λ_g, λ_s) and extinction (μ_g, μ_s) rates show sensitivity to spatial sampling extent and birth-death-sampling assumptions (Figs. 4, 5). In the results from PyRate, μ_g was virtually constant from the Devonian to the Capitanian stage of the Middle Permian. In the total dataset, μ_g increased twofold at the end of the Capitanian and continued to rise through the remainder of the Permian and into the Early Triassic, while in the spatially standardised dataset, a sixfold increase took place at the end of the Changhsingian across the Permian-Triassic boundary. In the complete dataset, λ_g was constant through the Devonian, then sharply decreased in the early Tournaisian into a period of constancy punctuated by a weak, transient increase at the end of the Carboniferous, then sharply increased threefold in Lopingian (Fig. 4D). After spatial standardisation, the sharp decrease in λ_g instead took place across the Devonian-Carboniferous boundary (Fig. 4D). The net result of these processes was a piecewise downshift in positive mean diversification rate from the Devonian into the Carboniferous, transient increases at the end of the Carboniferous and the Early Permian, then an increasingly negative rate through the Lopingian (Fig. 4F).

Species-level rates from PyRate are more volatile than at the genus level. μ_s declined gently from the Devonian to the middle of the Tournaisian, followed by steeper decline in the late Visean, then a sudden increase in the late Visean to a higher background rate. μ_s then spiked in the Moscovian before declining steadily to Devonian levels in the Early Permian, before a final spike though the Late Permian. (Fig. 4B). After spatial standardisation, μ_s rose through the Early and Middle Devonian and declined through the Late Devonian into the early Tournaisian, then followed the unstandardised pattern through the remainder of the Carboniferous. Standardised μ_s declined to a similar level in the Early Permian, but slightly later than in the unstandardised analyses, then spiked sharply at the Permian-Triassic

boundary (Fig 4B). Unstandardised and standardised λ_s shows similar patterns to those for μ_s through the Early Devonian to the late Serpukhovian and are similar to each other until the end of the Carboniferous. A transient pulse of speciation took place in the Bashkirian, before a sustained rate increase from the Moscovian into the earliest Permian. The unstandardised rate then slowly returned to Devonian levels by the Kungurian stage of the Early Permian, while the standardised rate dropped more sharply in the Asselian, but to a higher background rate. In both analyses, μ_s showed a small pulse at the end of the Early Permian, before dropping below Devonian rates in the Middle Permian, then spiked again in the Changhsingian (Fig. 4D). The overall result was a diversification rate which increased very gradually through the Devonian, then fluctuated between positive and negative regimes from the Carboniferous onwards (Fig. 4F).

PyRate found no evidence for a statistically significant increase in diversification rate at the Devonian-Carboniferous boundary at either the genus or species levels before or after spatial standardisation (Figs. 4B–4D, 4B–4D). Instead, diversification rates generally showed a modest decline at the onset of the Carboniferous (Figs. 5E–5F), driven by a statistically significant decrease in origination rate, an elevated rate in the late Pennsylvanian driven by elevated origination, and a sharp decline towards the end of the Permian driven by a statistically significant increase in extinction rate. Statistically significant rate shifts in origination and extinction are more prevalent at the species level compared to the genus level. Statistically significant rate shifts were also more prevalent after spatial standardisation, but many of these rate shifts are merely positive rather than strong and of negligible magnitude. Exceptions to this re spikes in the 95% highest posterior density in λ_s in the Serpukhovian and the end of the Kungurian, although the change in mean rate is again minimal (Fig. 5D).

Origination and extinction rates from RevBayes are more dynamic than those from PyRate and display greater uncertainty. (Figs. 4, 5). μ_g declined gently through the Early and Middle Devonian, fluctuated through the Late Devonian, rose then fell in the Tournaisian and Visean respectively, rose and fell again at the beginning of the Pennsylvannian epoch of the Carboniferous, then continued to rise for the remainder of the Carboniferous and into the Early Permian (Fig. 4A). μ_g dropped again at the end of the Late Permian, spiked in the Wuchiapingian, then spiked even more strongly across the Permian-Triassic boundary. These trends remain after spatial standardisation, apart from a more rapid rise in μ_g through the Pennsylvanian, then a more sudden decline in the Early Permian (Fig. 4A). In contrast to

extinction, λ_g showed stepwise increases through the Early and Middle Devonian, a drop in the Frasnian stage of the Late Devonian, a spike in the Fammenian stage at the end of the Devonian, then another decline in the Tournaisian (Fig. 4C). λ_g rose slightly during the Visean, then decreased to Early Devonian levels through the remainder of the Carboniferous and into the Early Permian (Fig. 4C). Spikes in origination punctuated the Kungurian and Wordian stages of the Early and Middle Permian respectively, but rates remained generally low otherwise (Fig. 4C). Trends are again largely unchanged following spatial standardisation, aside for a continued stepwise rate increase through the Devonian. These rates resulted in intervals of strongly positive diversification in the Middle Devonian, Fammenian, Visean and Kungurian, diversification close to zero in the Tournaisian, and further fluctuations between positive and negative regimes through the remainder of the Palaeozoic until a crash at the end of the Permian (Fig. 4E). Species-level dynamics from RevBayes show similar trends to those at genus level with more prominent spikes in origination and extinction rates, although the absolute magnitudes of species-level rates are generally lower than those recovered by PyRate (Fig. 5), and the timing of rate increases and decreases for μ_s in the Pennsylvanian are concordant before and after spatial standardisation, with a peak in extinction rates centred in the Asselian (Fig. 5A).

Bayes Factor tests marked very few RevBayes rate shifts as statistically significant. At the genus level, the only significant extinction rate shifts took place at the end of the Permian, but the timing of individual shifts are discordant before and after spatial standardisation (Fig. 4A), while significant shifts were also detected after spatial standardisation around the Permian-Carboniferous boundary at the species level. Following spatial standardisation, significant decreases in λ_g took place at the end of the Devonian, and at the ends of the Early and Middle Permian (Fig. 4C), while a significant increase took place at the beginning of the Kungurian. As with PyRate, species level rate shifts are more prevalent. Shifts in extinction rate following spatial standardisation were detected at the beginning and end of the Permian (Fig. 5A), while shifts in origination rate are dispersed through the Devonian, Mississippian and Kungurian (Fig. 5C).

4. Discussion

4.1 Actinopterygian diversity and sampling patterns. Our expanded occurrence database, incorporating all early actinopterygian taxa described to date, clarifies that diversification and sampling patterns recovered by previous analysis of the Palaeozoic actinopterygian fossil record [1,7] are subject to substantial geographic nuance. Sampling signal is overwhelmingly driven by low palaeolatitude occurrences from present day Europe and North America. Therefore, even our spatially broadest analyses return a signal that is primarily representative of actinopterygian diversity across Euramerica. Our diversity analyses at other spatial scales show that mid latitude trends may differ to those at lower, predominantly Euramerican latitudes, although the relative paucity of mid latitude assemblages makes it difficult to distinguish the extent to which these trends are truly biological or simply reflect temporal variation in sampling intensity. Consequently, it is not strictly possible to identify global trends in actinopterygian diversity, necessitating the potentially flawed assumption that the diversity patterns within our spatially standardised window are representative of global dynamics as the largest available subsample of their total diversity pool.

Our results also indicate that the impacts of spatial sampling bias on actinopterygian diversity patterns varied through the Palaeozoic. Our standardised analyses focus on Euramerica, yet the oldest actinopterygian occurrences come from outside of this region and are themselves geographically disparate (the South China Block and Brazilian Paraná Basin [42-43]), even though actinopterygians must necessarily have originated in a discrete location before expanding their range. Similarly, these occurrences are from marine facies, but the oldest Euramerican actinopterygian, *Cheirolepis trailli* from the Middle Devonian, is known from lacustrine deposits of the Orcadian Basin of Scotland. Actinopterygians clearly dispersed widely early in their evolutionary history, including from the marine to the freshwater realm, yet there is essentially no fossil record of these transitions [17], highlighting the spatiotemporal sampling deficits that plague their early fossil record despite its broad spatial extent.

Raw actinopterygian diversity patterns through the Devonian and Carboniferous were largely unaffected by heavy exclusion of occurrences during even our most stringent spatial standardisation procedures (Figs. 1B–1C). At face value this might suggest that their fossil record during this interval is well sampled enough to adequately record their diversity patterns, despite fluctuation in sampling intensity and spatial extent, but a more realistic interpretation is that sampling patterns are so heavily biased towards Euramerica that even

spatially standardised subsamples of their total fossil record will yield the same apparent diversity trends. The only clear instances where global spatial extent appears to affect sampled diversity is in the early Visean and Moscovian (Figs. 1B–1D), and sharp crashes in diversity or diversification rates during this interval are not supported by SIB and CBR diversity trends from our hexagonally binned subsamples or our results from PyRate or RevBayes (Figs. 3A–3C, 4E–4F, 5E–5F). We therefore predict that future sampling of known or undiscovered early Visean localities should reveal greater actinopterygian diversity than is currently known.

Diversity patterns through the Permian are more challenging to interpret due to conflicting diversity signals between metrics and spatial scales. Sampling extent is higher through the Permian compared to the Carboniferous, corroborating previous findings [8] and correlating with generally high diversity throughout the period, although diversity is largely undiminished when sampling extent is subsequently controlled for (Figs. 1D–1E). High diversity in the Early Permian is also recovered by sampling-corrected metrics before and after spatial standardisation, but the estimates are abnormally high compared to the rest of the dataset (Figs. 1E–1F). A possible explanation for this is the taxonomic composition of the data in this interval. Extensive historical collection in deposits spanning the Asselian and Sakmarian stages of the Permian across Europe [44-46], combined with frequent taxonomic splitting of potentially synonymous specimens sampled from the East European and Siberian platforms may result in highly skewed abundance distributions during this interval. This sampling effect explains the unexpectedly high diversity estimates returned by CBR and SQR during this interval as these metrics show sensitivity to extremely uneven abundance distributions but is eliminated when mean local diversity patterns are examined (Figs. 3A–3C, 4A–4C). Reductions in low latitude local diversity in contrast to increases in mid latitude local diversity in the Early Permian lends circumstantial support to the hypothesis that reduction in the areas of equatorial coastal and freshwater environments during the assembly and aridification of Pangaea may have curtailed rising actinopterygian diversity [7] or at least in its well-sampled Euramerican component. Low latitude reductions in diversity did not persist through the remainder of the Permian, however, suggesting that while actinopterygian diversification may have been curtailed by the assembly of Pangaea, they remained locally successful components of marine and freshwater ecosystems. Careful study of taxon validity and specimen affiliations is required to ascertain reliable patterns of raw diversity in the Early Permian, however, before this hypothesis can be properly validated.

While actinopterygian diversity patterns can be partly isolated from variation in spatial sampling extent by focusing on the consistently sampled Euramerican region, this record may still be prone to other sources of bias, particularly the taphonomic effects of lagerstätten. Lagerstätte-bearing intervals may display inflated diversity estimates resulting from disproportionately complete preservation of past assemblages, with exceptional preservation additionally lending itself to increased potential for the recognition of taxonomically and phylogenetically diagnostic characters [47-48]. Consequently, Euramerican lagerstätten such as Mazon Creek or the Kinney Brick Quarry (late Moscovian and early Gzhelian respectively [49,50]) may still upward bias diversity estimates even after accounting for variation in sampling effort, although previous studies have noted that lagerstätten effects on diversity are spatially and taxonomically variable [51]. Conceivably, the role of lagerstatten in provisioning exceptionally preserved, character rich specimens [52] may also impact phylogenetic estimations of early actinopterygian diversification.

4.2 Actinopterygian diversification through mass extinction. The Late Devonian was affected by two mass extinction events, namely the Kellwasser event at the end of the Frasnian and the Hangenberg event at the end of the Famennian. Compared to the latter, the Kellwasser event had a more significant impact on reef ecosystems [53], of which actinopterygians were a part (e.g., the Frasnian Gogo Formation of Western Australia [20]). We find diminished actinopterygian diversity in the early Famennian compared to the Frasnian from both raw and sampling-corrected metrics before and after spatial standardisation (Fig. 1D). There is no evidence, however, for a significant increase in extinction rates at either the species or genus levels (Fig 4, 5), corroborating previous inferences that Kellwasser event had only a minor impact on vertebrate faunas [1]. More generally, it has been suggested that apparent impacts across other vertebrates represent backsmearing of lineage-wise extinctions due to poor sampling in the Famennian [1], but while occurrence counts for actinopterygians are indeed higher in the Frasnian, the spatial extent of Famennian occurrences is higher following spatial standardisation and trends in diversity are unchanged. Resolving the precise impacts of the Kellwasser event on actinopterygians will therefore necessitate section level analysis to avoid the confounding effects of spatiotemporal sampling biases.

Previous authors have posited that an explosive radiation of actinopterygians took place in the early Carboniferous [1,3]. We find, however, that while actinopterygian diversity did increase during this interval across a range of spatial scales, there is no statistical evidence for

a significant increase in diversification rate after the Hangenberg event. Discrepant evidence is also provided by these approaches for elevated diversification in the Late Devonian. PyRate returns only weak evidence for increased diversification rates in the Famennian (Fig. 4E, 5E), but the rise in diversity is apparent in the early Carboniferous (Fig. 1C–1F). This suggests that there must have been sufficient lineages present in the Devonian combined with high survivorship into the Carboniferous to facilitate rapid growth in diversity without any clear shifts in diversification rate. Our PyRate analyses indicate that the maximum true stratigraphic ranges of as many as 33 known actinopterygian taxa may have spanned the Devonian-Carboniferous boundary (Fig. 6), highlighting the potential extent of their cryptic diversification and survivorship prior to the Tournaisian. In some cases, this survivorship may be artefactual, arising from backwards extension of wastebasket taxa which share conservative fusiform morphologies. For example, the genera *Kentuckia* and *Gonatodus* are both recovered as boundary crossers, but species-level comparison between their respective Devonian and Carboniferous genera strongly suggests that they are polyphyletic [17,54]. In other cases, however, the boundary crossers display substantial morphological variation and are also geographically widespread and taxonomically disparate [1,55], suggesting that their survivorship and rapid morphological innovation are representative of the wider diversification dynamics that underpinned early actinopterygian success. Some early Carboniferous taxa retain Devonian-grade anatomy, showing that survivorship was not strictly coupled with morphological innovation [15]. The high morphological diversity and abundance displayed by actinopterygians in Tournaisian marine and freshwater deposits [1,55-57], along with evidence for Carboniferous-grade anatomies in some Late Devonian actinopterygians [12,58], further indicate that the rapid independent acquisitions of novel body forms across multiple lineages may have had roots predating the Hangenberg event.

PyRate is limited by its assumption of complete taxon sampling in its default birth-death model and so cannot infer the times at which lineages diverged within the wider, unobserved phylogeny of early actinopterygians, some of which may also have conceivably crossed the Devonian-Carboniferous boundary. RevBayes does not provide estimates of true lineage durations but can relax the assumption of complete species sampling during inference of origination and extinction rates. Results from this model support a statistically significant increase in genus and species origination rates in the Famennian before and after spatial standardisation, resulting in the elevated diversification rates needed to generate the cryptic diversity within the evolutionary scenario we propose here. Devonian actinopterygian

occurrence and taxon counts are still low, however, and so their relative scarcity through most of this interval appears genuine. There is a conspicuous drop in occurrence counts in the late Famennian following spatial standardisation, however, and so the impression of low diversity just prior to the Hangenberg event may also be an artefact of poor sampling. Indeterminate fragments of actinopterygians present in Late Devonian and early Carboniferous deposits are also suggestive of their unappreciated taxonomic diversity during this critical interval in their early history [56,59,60]. In turn, future description of actinopterygian taxa in the Famennian or improved sampling of early Carboniferous taxa in phylogenetic trees is expected to address this deficit, particularly given the relative understudy of small bodied, poorly preserved specimens from the Late Devonian, some of which evidence the earlier acquisition of Carboniferous-grade morphologies [58].

Results from PyRate and RevBayes both indicate cryptic diversification during the Late Devonian, with respective decreases and increase in origination and extinction rates in the early Carboniferous. This corroborates recent phylogenetically-derived suggestions that the recognition of diverse, morphologically distinct actinopterygian lineages in the Carboniferous is predicated on anatomical divergences and lineage separations rooted in the Late Devonian [12]. These patterns suggest that competitive exclusion by other gnathostome clades may not have been a prevalent mechanism shaping early actinopterygian diversity patterns, as suppression of origination rates would be the expected outcome. Instead, the decline in origination rates may reflect increasing intraclade competition as actinopterygians increased in abundance and diversity into the Carboniferous. The increase in extinction rates in the same interval may be a passive component of their increasing diversity as the number of lineage terminations will still rise even if proportional extinction rates remain constant. Conceivably, however, it could also reflect a slight increase in extinction risk in within actinopterygian lineages which developed specialist morphologies and lifestyles with a naturally greater degree of environmental sensitivity.

5. Conclusions

Birth-death modelling does not support exceptional shifts in actinopterygian diversification rates in the early Carboniferous, but sampling-corrected diversity patterns robustly support a marked increase in the number of actinopterygian taxa during this interval. A solution to this

apparent contradiction is cryptic diversification of actinopterygians in the Late Devonian coupled with high lineage survivorship across the Hangenberg event. If this scenario is accurate, then formal phylogenetic analyses incorporating a greater proportion of the total known diversity of Palaeozoic actinopterygians and improved sampling of their Famennian fossil record should recover these early divergences. Additionally, cryptic diversification and poor sampling during the Famennian are not mutually exclusive explanations for the apparent disconnect between elevated diversification in the Late Devonian and elevated diversity in the Tournaisian, as a response lag between an increase in rate and its resultant product may be further exacerbated when the latter is also undersampled. Complex taxonomic histories and imprecise assignment of numerous actinopterygian specimens to wastebasket taxa likely masks a more substantial pool of Palaeozoic species diversity than is currently appreciated, while overzealous splitting of anatomically identical specimens will conversely overinflate diversity estimates. Future analytical gain will therefore come from taxonomic resolution of these wastebaskets and improved sampling of their Famennian fossil record.

Regime shifts in actinopterygian diversity at local, regional, and continental scales observed in the early Carboniferous nonetheless mark the Hangenberg event as a turning point in their macroevolutionary history, with Carboniferous actinopterygians showing wider geographic distributions and ecomorphological diversity compared to in the Devonian [2]. Their increase in taxonomic diversity may not have been driven by exceptional diversification rates, but their change in ecological prominence was still profound. An explanation for this is high survivorship of morphologically conservative, cryptic Devonian taxa coupled with their ecological release during the Hangenberg event resulting in the decoupling of taxonomic and ecological diversity, a pattern which is seen elsewhere in the fossil record across mass extinction boundaries (e.g., [61]). Conversely, there is evidence that many of the survivors may have displayed higher morphological diversity than is currently appreciated. Future work should therefore also focus on characterising patterns of actinopterygian morphospace and ecospace occupancy from the Devonian to the Carboniferous to ascertain how ecological release versus intraclade competition may have shaped their subsequent evolutionary radiation.

References

1. Sallan L, Coates M. (2010). End-Devonian extinction and a bottleneck in the early evolution of modern jawed vertebrates. *P. Natl. Acad. Sci. USA.* **107**, 10131–10135.
2. Friedman M. (2015). The early evolution of ray-finned fishes. *Palaeontology* **58**, 213–228.
3. Sallan, L., Friedman, M. (2011). Heads or tails: staged diversification in vertebrate evolutionary radiations. *P. R. Soc. B.* **289**, 279, 2025–2032.
4. Zhu M, Zhao W, Jia L, Lu J, Qiao T, Qu Q. (2009). The oldest articulated osteichthyan reveals mosaic gnathostome characters. *Nature* **458**, 469–474.
5. Giles S, Friedman M., Brazeau, M. (2015). Osteichthyan-like cranial conditions in an Early Devonian stem gnathostome. *Nature* **520**, 82–85.
6. Schultze H, Mickle K, Poplin C, Hilton E, Grande L. (2021). *Handbook of Paleoichthyology, Volume 8A: Actinopterygii I.* Verlag Dr Friedrich Pfeil, Munich. 299p.
7. Friedman M, Sallan L. (2012). Five hundred million years of extinction and recovery: a Phanerozoic survey of large-scale diversity patterns in fishes. *Palaeontology* **55**, 707–742.
8. Henderson S, Dunne E, Giles S. (2022). Sampling biases obscure the early diversification of the largest living vertebrate group. *P. R. Soc. B.* **289**, 20220916.
9. Henderson S, Dunne E, Fasey S, Giles S. (2022). The early diversification of ray-finned fishes (Actinopterygii): hypotheses, challenges and future prospects. *Biol. Rev.* **98**, 284–315.
10. Clement A, King B, Giles S, Choo B, Ahlberg P, Young G, Long J. (2018). Neurocranial anatomy of an enigmatic Early Devonian fish sheds light on early osteichthyan evolution. *eLife* e34349.
11. Giles S, Xi G, Near T, Friedman M. (2017). Early members of ‘living fossil’ lineage imply later origin of modern ray-finned fishes. *Nature* **549**, 265–268.

12. Giles S, Feilich K, Warnock R, Piece S, Friedman M. (2023). A Late Devonian actinopterygian suggests high lineage survivorship across the end-Devonian mass extinction. *Nat. Ecol. Evol.* **7**, 10–19.
13. Caron A, Venkataraman V, Tietjen K, Coates M. (2023). A fish for Phoebe: a new actinopterygian from the Upper Carboniferous Coal Measures of Saddleworth, Greater Manchester, UK, and a revision of *Kansasiella eatoni*. *Zool. J. Linn. Soc Lond.* **198**, 957–981
14. Sallan L, Galimberti A. (2015). Body-size reduction in vertebrates following the end-Devonian mass extinction. *Science* **350**, 812–815.
15. Wilson C, Pardo J, Anderson J. (2018). A primitive actinopterygian braincase from the Tournaisian of Nova Scotia. *R. Soc. Open Sci.* **5**, 171727.
16. Sallan L. (2014). Major issues in the origins of ray-finned fish (Actinopterygii) biodiversity. *Biol. Rev.* **89**, 950–971.
17. Friedman M, Blom H. (2006). A new actinopterygian from the Famennian of East Greenland and the interrelationships of Devonian ray-finned fishes. *J. Palaeontol.* **80**, 1186–1204.
18. Long J, Choo B, Young G. (2008). A new basal actinopterygian fish from the Middle Devonian. *Antarct. Sci.* **20**, 393–412.
19. Choo B, Long J, Trinajstic K. (2009). A new genus and species of basal actinopterygian fish from the Upper Devonian Gogo Formation of Western Australia. *Acta Zool.* **90**, 194–210.
20. Choo B. (2012). Revision of the actinopterygian genus *Mimipiscis* (=*Mimia*) from the Upper Devonian Gogo Formation of Western Australia and the interrelationships of the early Actinopterygii. *Earth Env. Sci. T. R. So.* **102**, 77–104.
21. Giles S, Darras L, Clément G, Blieck A, Friedman M. (2015). An exceptionally preserved Late Devonian actinopterygian provides a new model for primitive cranial anatomy in ray-finned fishes. *P. R. Soc. B* **282**, 20151485.
22. Li J, Huang J, Sukumaran J, Knowles L. (2018). Microevolutionary processes impact macroevolutionary patterns. *BMC Evol. Biol.* **18**, 123.
23. Close R, Benson R, Upchurch P, Butler R. (2017). Controlling for the species-area effect supports constrained long-term Mesozoic terrestrial vertebrate diversification. *Nat. Commun.* **8**, 15381.
24. Close R, Benson R, Saupe E, Clapham M, Butler R. (2020). The spatial structure of Phanerozoic marine animal diversity. *Science* **368**, 420–424.

25. Close R, Benson R, Alroy J, Carrano M, Cleary T, Dunne E, Mannion P, Uhen M, Butler R. (2020). The apparent exponential radiation of Phanerozoic land vertebrates is an artefact of spatial sampling biases. *P. R. Soc. B* **287**, 20200372.
26. Flannery-Sutherland J, Silvestro D, Benton M. (2022). Global diversity dynamics in the fossil record are regionally heterogeneous. *Nat. Commun.* **13**, 2751.
27. Flannery-Sutherland J, Crossan C, Myers C, Hendy A, Landman N, Witts J. (2024). Late Cretaceous ammonoids show that drivers of diversification are regionally heterogeneous. *Nat. Commun.* **15**, 5382.
28. Antell G, Benson R, Saupe E. (2024). Spatial standardization of taxon occurrence data – a call to action. *Paleobiology* **50**, 177–193.
29. Allen, B., Clapham, M., Saupe, E., Wignall, P., Hill, D., Dunhill, A. (2023). Estimating spatial variation in origination and extinction in deep time. *Paleobiology* **49**, 509–526.
30. Silvestro D, Salamin N, Schnitzler J. (2014). PyRate: a new program to estimate speciation and extinction rates from incomplete fossil data. *Meth. Ecol. Evol.* **5**, 1126–1131.
31. Silvestro D, Schnitzler J, Li L, Antonelli, A., Salamin, N. (2014). Bayesian estimation of speciation and extinction from incomplete fossil occurrence data. *Syst. Biol.* **63**, 349–367.
32. Silvestro D, Salamin N, Antonelli A, Meyer X. (2019). Improved estimation of macroevolutionary rates from fossil data using a Bayesian framework. *Paleobiology* **45**, 546–570.
33. Stadler T, Gavryushkina A, Warnock R, Drummond A, Heath T. (2018). The fossilized birth-death model for the analysis of stratigraphic range data under different speciation modes. *J. Theor. Biol.* **447**, 41–55.
34. Dean C, Chiarenza A, Maidment S. (2020). Formation binning: a new method for increased temporal resolution in regional studies, applied to the Late Cretaceous dinosaur fossil record of North America. *Palaeontology* **63**, 881–901
35. Benson R, Butler R, Close R, Saupe E, Rabosky D. (2021). Biodiversity across space and time in the fossil record. *Curr. Biol.* **31**, R1225–R1236.
36. Hendricks J, Saupe E, Myers C, Hermsen E, Allmon W. (2016). The generification of the fossil record. *Paleobiology* **40**, 511–528.
37. Alroy, J. (2014). Accurate and precise estimates of origination and extinction rates. *Paleobiology* **40**, 374–397.
38. Alroy J. (2015). A more precise speciation and extinction rate estimator. *Paleobiology* **41**, 633–639.

39. Warnock R, Heath T, Stadler T. (2020). Assessing the impact of incomplete species sampling on estimates of speciation and extinction rates. *Paleobiology* **46**, 137–157.
40. Pett W, Warnock R, Gavryushkina A. (2022). Macroevolutionary analysis of stratigraphic range data. RevBayes tutorial (accessed 25/04/24). https://revbayes.github.io/tutorials/fbd_range/FBD_skyline_maths.pdf.
41. Höhna S, Landis M, Heath T, Boussau B, Lartillot N, Moore B, Huelsenbeck J, Ronquist F. (2016). RevBayes: Bayesian phylogenetic inference using graphical models and an interactive model-specification language. *Syst. Biol.* **65**, 726–736.
42. Lu J, Giles S, Friedman M, den Blaauwen J, Zhu M. (2016). The oldest actinopterygian highlights the cryptic early history of the hyperdiverse ray-finned fishes. *Curr. Biol.* **26**, 1602–1608.
43. Figueroa R, Weinschültz L, Friedman M. (2021). The oldest Devonian circumpolar ray-finned fish? *Biol. Lett.* **17**, 20200766.
44. Stamberg S. (2006). Carboniferous-Permian actinopterygian fishes of the continental basins of the Bohemian Massif, Czech Republic: an overview. *Geol. Soc. Lond. Spec. Publ.* **265**, 217–230.
45. Stamberg S. (2013). Knowledge of the Carboniferous and Permian actinopterygian fishes of the Bohemian Massif – 100 years after Antonín Frič. *Acta Mus. Nat. Pragae, Ser. B* **69**, 159–181.
46. Stamberg S. (2018). Actinopterygians of the Permian locality Buxières-Les-Mines (Bourbon l'rchambault Basin, France) and their relationship to other early actinopterygians. *Foss. Imp.* **74**, 245–291.
47. Benson R, Butler R. (2011). Uncovering the diversification history of marine tetrapods: ecology influences the effect of geological sampling biases. *Geol. Soc. Lond. Spec. Publ.* **358**, 191–208.Benson R, Butler R, Close R, Saupe E, Rabosky D. (2021). Biodiversity across space and time in the fossil record. *Curr. Biol.* **31**, R1225–R1236.
48. Dean C, Mannion P, Butler R. (2016). Preservational bias controls the fossil record of pterosaurs. *Palaeontology* **59**, 225–247.
49. Clements T, Purnell M, Gabbott S. (2018). The Mazon Creek lagerstätte: a diverse late Paleozoic ecosystem entombed within siderite concretions. *J. Geol. Soc.* **176**, 1–11.
50. Lucas S, Dimichele W, Allen B. (2021). The Kinney Brick Quarry lagerstätte, late Pennsylvanian of New Mexico, USA: introduction and overview. *Bull. N. M. Mus. Nat. Hist. Sci.* **84**, 1–16

51. Walker F, Dunhill A, Benton M. (2019). Variable preservation potential and richness in the fossil record of vertebrates. *Palaeontology* **63**, 313–329.
52. Woolley C, Bottjer D, Corsetti F, Smith N. (2024). Quantifying the effects of exceptional fossil preservation on the global availability of phylogenetic data in deep time. *PLoS ONE* **19**, e0297637
53. Carmichael S, Waters J, Königshof P, Suttner T, Kido E. (2019). Paleogeography and paleoenvironments of the Late Devonian Kellwasser event: a review of its sedimentological and geochemical expression. *Global Planet. Change* **183**, 102984.
54. Igielman B, Figueroa R, Higgins R, Pierce S, Coates M, Troyer E, Fernandez V, Dollman K, Lu J, Zhu M, et al. (2025). The lower jaw of Devonian ray-finned fishes (Actinopterygii): anatomy, relationships, and functional morphology. Preprint at biorxiv.org/content/10.1101/2025.01.30.635695v1.full.
55. Holland T, Long J, Warren A, Garvey J. (2006). Second specimen of the lower actinopterygian *Novogonatodus kasantsevae* Long 1988 from the Early Carboniferous of Mansfield, Victoria. *P. R. Soc. Victoria* **118**, 1–10.
56. Clack J, Bennett C, Davies S, Scott A, Sherwin J, Smithson T. (2019). A Tournaisian (earliest Carboniferous) conglomerate-preserved non-marine faunal assemblage and its environmental and sedimentological context. *PeerJ* **3**, e5972.
57. Wilson C, Mansky C, Anderson J. (2021). A platysomid occurrence from the Tournaisian of Nova Scotia. *Sci. Rep. UK.* **11**, 8375
58. Janvier P, Lethiers F, Monod O, Balkaş Ö. (1984). Discovery of a vertebrate fauna at the Devonian-Carboniferous Boundary in SE Turkey (Hakkari Province). *J. Petrol. Geol.* **7**, 47–168.
59. Blieck A, Goujet D, Janvier P. (1987). The vertebrate stratigraphy of the Lower Devonian (Red Bay Group and Wood Bay Formation) of Spitsbergen. *Mod. Geol.* **1**, 197–217.
60. Plax D. (2022). A new species of the ray-finned fish (Osteichthyes, Actinopterygii) from the upper Emsian and lowermost Eifelian deposits of Belarus. *Lithosphere* **1**, 30–39.
61. Ruta M, Angielczyk K, Fröbisch J, Benton M. (2013). Decoupling of morphological disparity and taxic diversity during the adaptive radiation of anomodont therapsids. *P. R. Soc. B.* **280**, 20132414.

Acknowledgements

S.G, J.F.S. and S.F. were funded by a Royal Society Dorothy Hodgkin Research Fellowship (DH160098) to S.G. S.H was funded by a Royal Society Enhancement Award to S.G. (grant no. RGF\EA\180279). We thank Emma Dunne, Richard Butler and Matt Friedman for helpful discussions.

Author contributions

J.F.S and S.G conceived the study. S.H compiled the actinopterygian database at the core of this work which was expanded by J.F.S. J.F.S and S.F uploaded the occurrences to the PBDB. J.F.S carried out all analyses and wrote the manuscript with input from all authors.

Data availability

All fossil occurrence data used in this work is publicly available through the PBDB. All code scripts and data used to run our analyses are available in the paper electronic supplement (10.6084/m9.figshare.28789472). PyRate and RevBayes are freely available online (https://github.com/dsilvestro/PyRate; https://revbayes.github.io/download).

Figure 1. Global properties of the Palaeozoic actinopterygian fossil occurrence record. Properties were calculated in ~3 Ma intervals from all occurrences, occurrences subsampled in a discrete spatial window, and occurrences additionally subsampled to an even geographic extent by their minimum spanning tree length. Grey bars demarcate the stages of the Phanerozoic. Vertical dashed lines indicate end of period. Coloured ribbons demarcate the epochs of the Phanerozoic, aside from in the Carboniferous where stage-level divisions of the Mississippian and Pennsylvanian are displayed. **A.** Number of fossil occurrences through time. **B.** Geographic extent of fossil occurrences measured as the length of their minimum spanning tree. **C.** Raw actinopterygian genus diversity sampled in each time bin. **D.** Actinopterygian genus diversity inferred from observed stratigraphic ranges. **E.** Sampling standardised actinopterygian diversity estimated by coverage-based rarefaction. **F.** Sampling standardised actinopterygian diversity estimated by Squares extrapolation.

Figure 2. Palaeozoic actinopterygian diversity across latitudes. Diversity was calculated in ~3 Ma intervals in low (0°–30°; A, D, G, J), medium (30°–60°; B, E, H, K) and high (6°–90°; C, F, I, L) absolute palaeolatitude bins, using sampled-in-bin (A–D), range-through-time (D–F), coverage-based rarefaction (G–I) and Squares extrapolation (J-K) metrics, from all occurrences (raw), occurrences subsampled in a discrete spatial window (windowed), and occurrences additionally subsampled to an even geographic extent (MST-standardised). Coloured ribbons demarcate the epochs of the Phanerozoic, aside from in the Carboniferous where stage-level divisions of the Mississippian and Pennsylvanian are displayed. Vertical dashed lines indicate end of period

Figure 3. Local Palaeozoic actinopterygian diversity trends. Diversity was calculated from collections of actinopterygian fossil occurrences aggregated into equal area grid cells, using sampled-in-bin (A, D, G, J), coverage-based rarefaction (B, E, H, K) and Squares extrapolation (C, F, I, L) diversity metrics. Mean and median trends were then calculated from all collections (A–C), and from collections divided into low (0°–30°; D–F), medium (30°–60°; G–I) and high (6°–90°; J – L) absolute palaeolatitude bins. Y axes have been log transformed for clarity. Coloured ribbons demarcate the epochs of the Phanerozoic, aside from in the Carboniferous where stage-level divisions of the Mississippian and Pennsylvanian are displayed. Vertical dashed lines indicate end of period

Figure 4. Genus-level diversification dynamics of Palaeozoic actinopterygians. Origination (λ_g) and extinction (μ_g) rates, resultant net diversification rates, and 95% highest posterior densities were estimated under two different birth-death-sampling processes using Bayesian inference. Results in colour are from the total dataset, while results in grey are from a subsample of the dataset following spatial standardisation by minimum spanning tree length. Statistical support for the significance of extinction and origination rate shifts is displayed at the bottom of each plot. Grey bars demarcate the stages of the Phanerozoic. Vertical dashed lines indicate end of period. Coloured ribbons demarcate the epochs of the Phanerozoic, aside from in the Carboniferous where stage-level divisions of the Mississippian and Pennsylvanian are displayed. **A.** Genus extinction rate from RevBayes. **B.** Genus extinction rate from PyRate. **C.** Genus origination rate from RevBayes. **D.** Genus origination rate from PyRate. **E.** Genus diversification rate from RevBayes. **F.** Genus diversification rate from PyRate.

Figure 5. Species-level diversification dynamics of Palaeozoic actinopterygians. Origination (λ_s) and extinction (μ_s) rates, resultant net diversification rates, and 95% highest posterior densities were estimated under two different birth-death-sampling processes using Bayesian inference. Results in colour are from the total dataset, while results in grey are from a subsample of the dataset following spatial standardisation by minimum spanning tree length. Statistical support for the significance of extinction and origination rate shifts is displayed at the bottom of each plot. Grey bars demarcate the stages of the Phanerozoic. Vertical dashed lines indicate end of period. Coloured ribbons demarcate the epochs of the Phanerozoic, aside from in the Carboniferous where stage-level divisions of the Mississippian and Pennsylvanian are displayed. **A.** Species extinction rate from RevBayes. **B.** Species extinction rate from PyRate. **C.** Species origination rate from RevBayes. **D.** Species origination rate from PyRate. **E.** Species diversification rate from RevBayes. **F.** Species diversification rate from PyRate.

Figure 6. Stratigraphic ranges of actinopterygian taxa spanning the Hangenberg event. Sampling-corrected stratigraphic ranges were estimated using PyRate. The vertical dotted lines mark timing of the Kellwasser and Hangenberg events at Frasnian-Famennian and the Devonian-Carboniferous boundaries respectively. Coloured ribbons demarcate the epochs of the Phanerozoic, aside from in the Carboniferous where stage-level divisions of the Mississippian and Pennsylvanian are displayed.

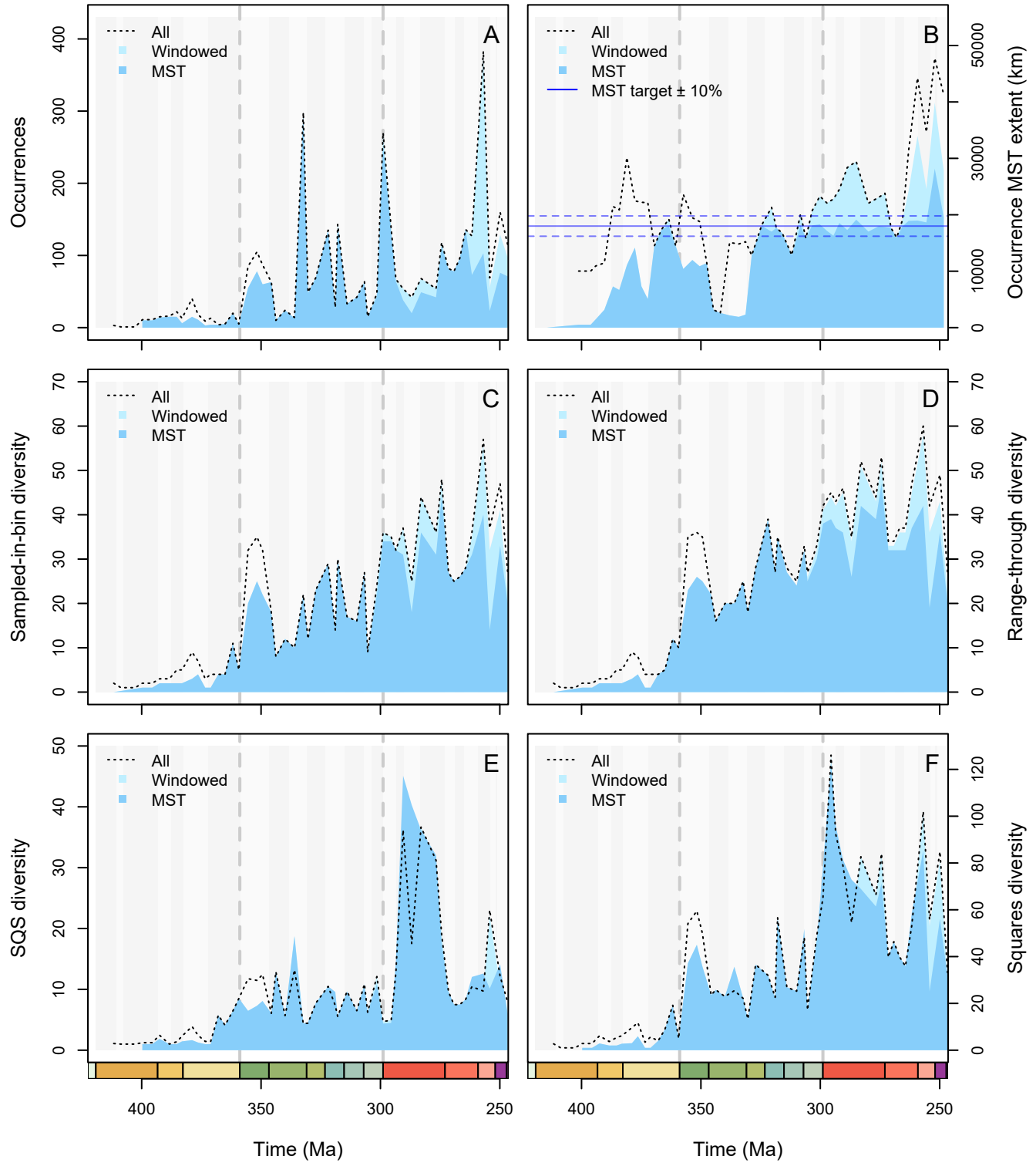
A
B
C
D
E
F
All
Windowed
MST
MST target ± 10%
Occurrences
Occurrence MST extent (km)
Sampled-in-bin diversity
Range-through diversity
SQS diversity
Squares diversity
Time (Ma)
400
350
300
250

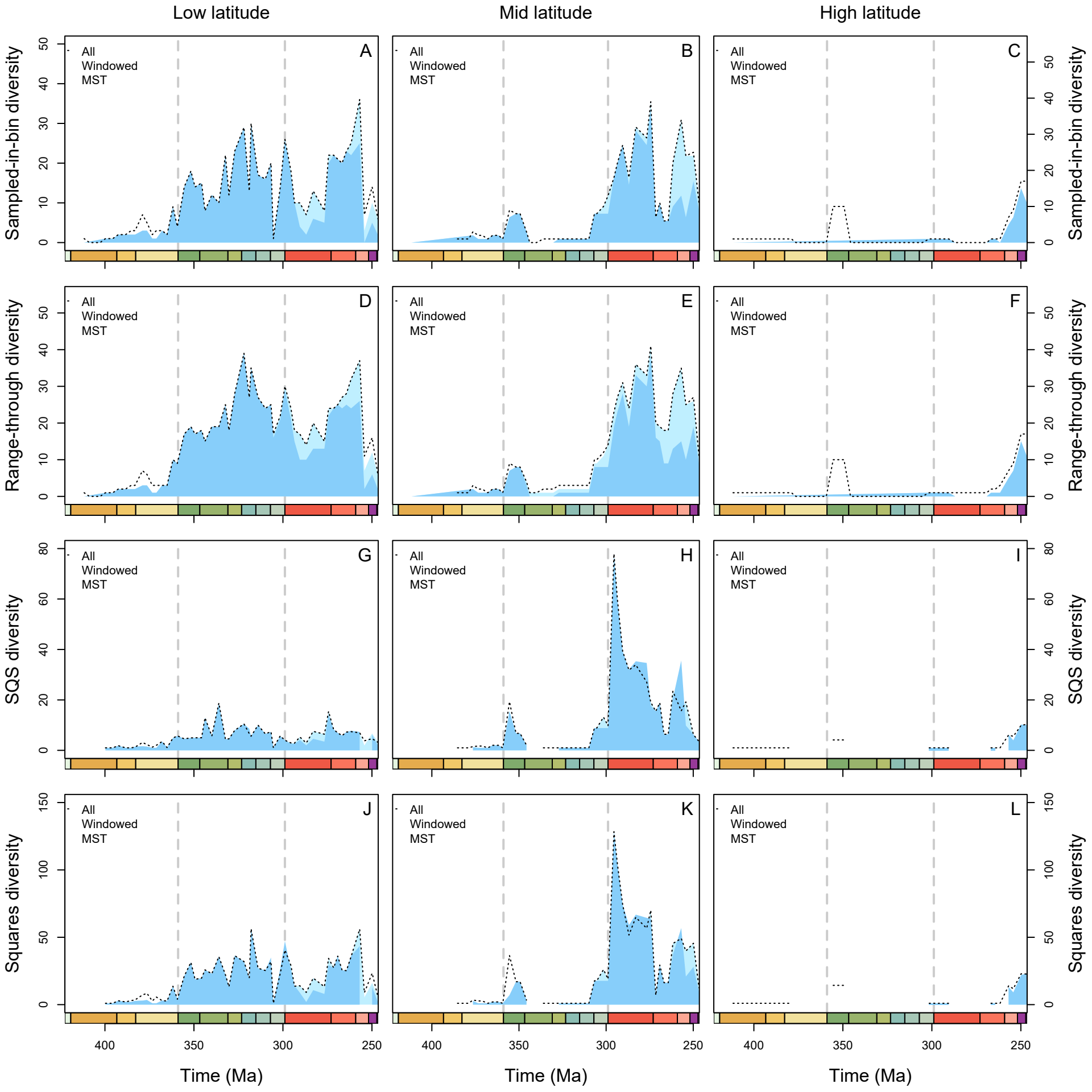
Low latitude
Mid latitude
High latitude
Sampled-in-bin diversity
Range-through diversity
SQS diversity
Squares diversity
All
Windowed
MST
A
B
C
D
E
F
G
H
I
J
K
L
Time (Ma)
400
350
300
250

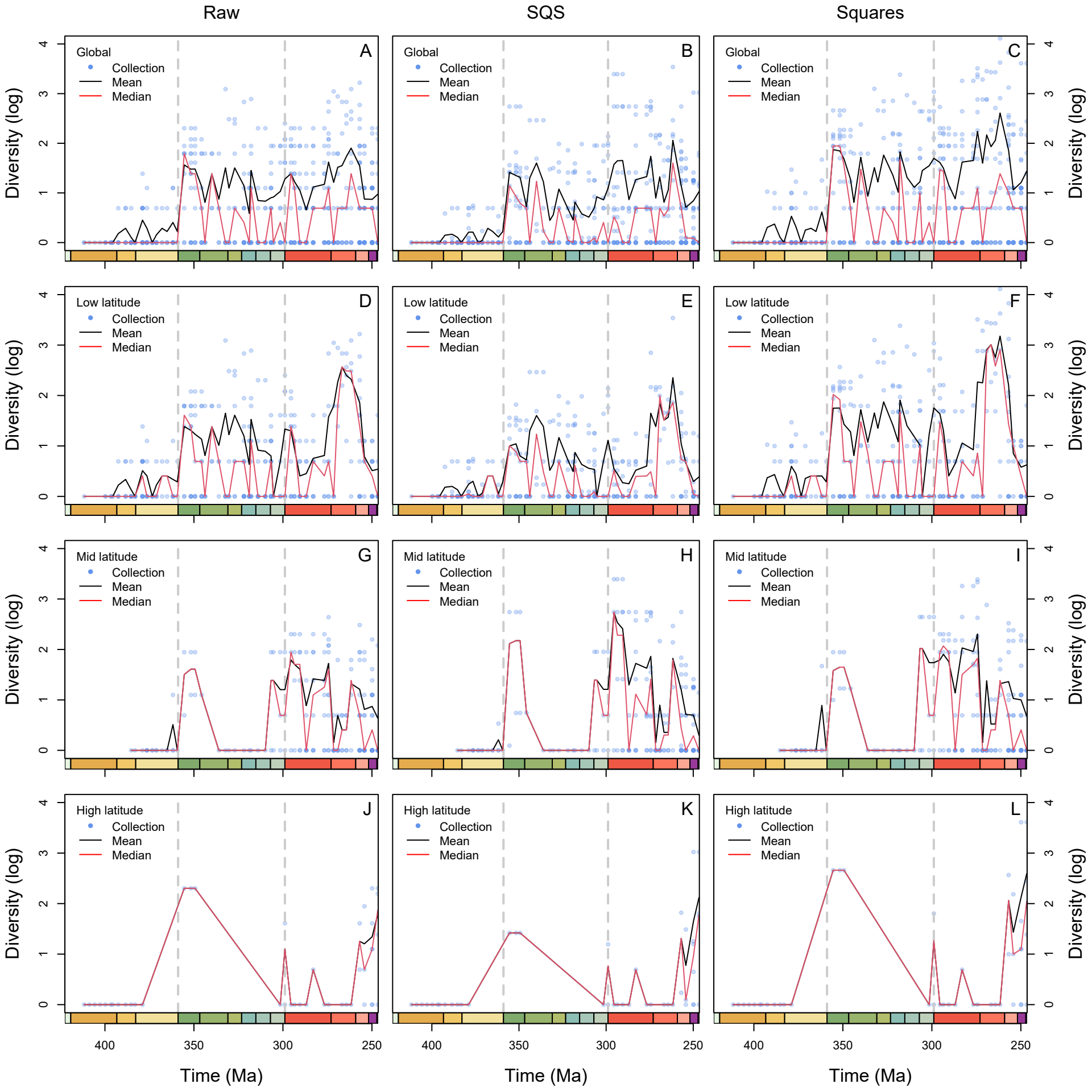
Raw
SQS
Squares
Global
Low latitude
Mid latitude
High latitude
Collection
Mean
Median
A
B
C
D
E
F
G
H
I
J
K
L
Diversity (log)
Time (Ma)
400
350
300
250

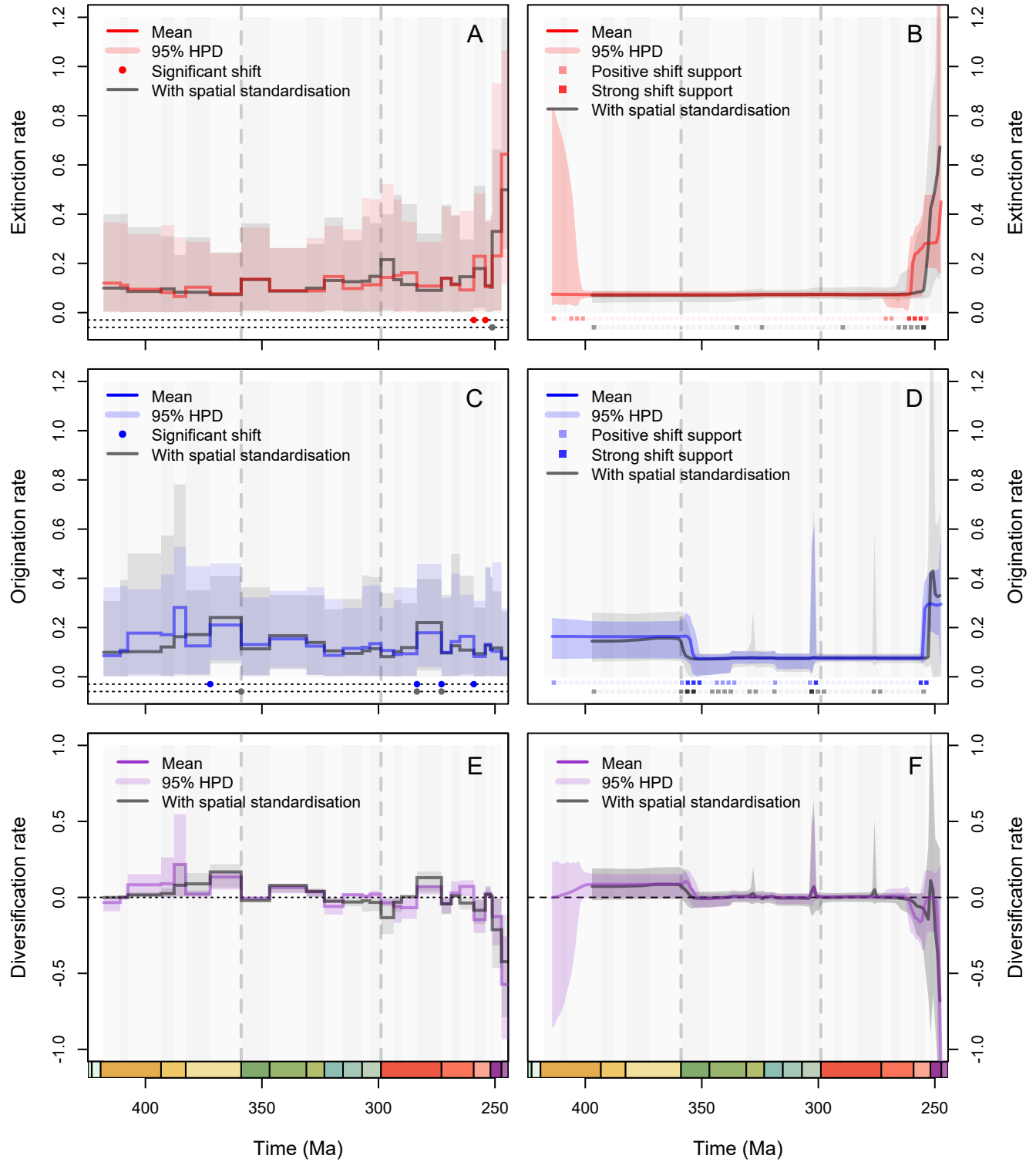
A
Mean
95% HPD
Significant shift
With spatial standardisation
Extinction rate
B
Mean
95% HPD
Positive shift support
Strong shift support
With spatial standardisation
Extinction rate
C
Mean
95% HPD
Significant shift
With spatial standardisation
Origination rate
D
Mean
95% HPD
Positive shift support
Strong shift support
With spatial standardisation
Origination rate
E
Mean
95% HPD
With spatial standardisation
Diversification rate
F
Mean
95% HPD
With spatial standardisation
Diversification rate
400
350
300
250
Time (Ma)
Time (Ma)

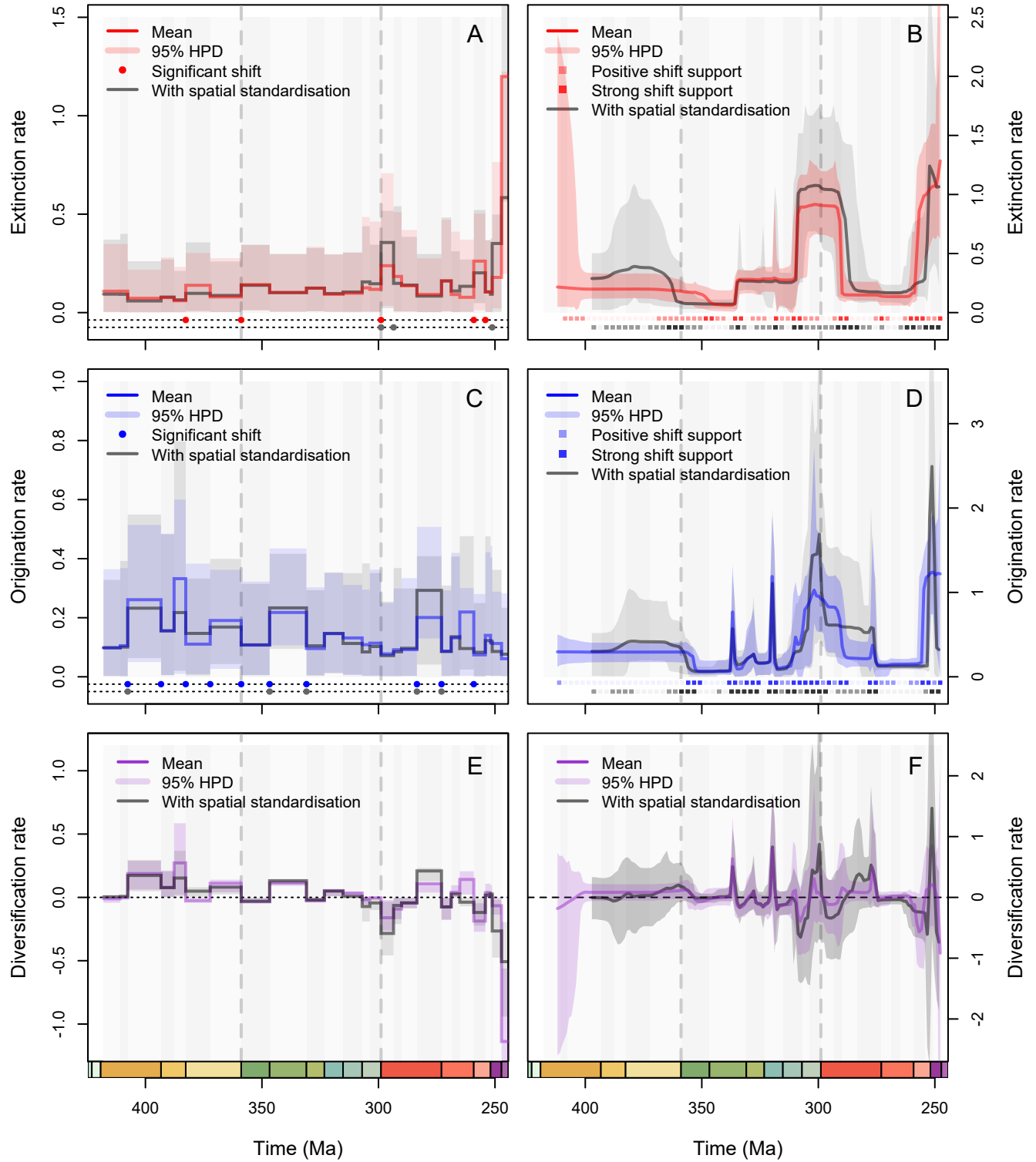
A
Mean
95% HPD
Significant shift
With spatial standardisation
Extinction rate
B
Mean
95% HPD
Positive shift support
Strong shift support
With spatial standardisation
Extinction rate
C
Mean
95% HPD
Significant shift
With spatial standardisation
Origination rate
D
Mean
95% HPD
Positive shift support
Strong shift support
With spatial standardisation
Origination rate
E
Mean
95% HPD
With spatial standardisation
Diversification rate
F
Mean
95% HPD
With spatial standardisation
Diversification rate
400
350
300
250
Time (Ma)
Time (Ma)

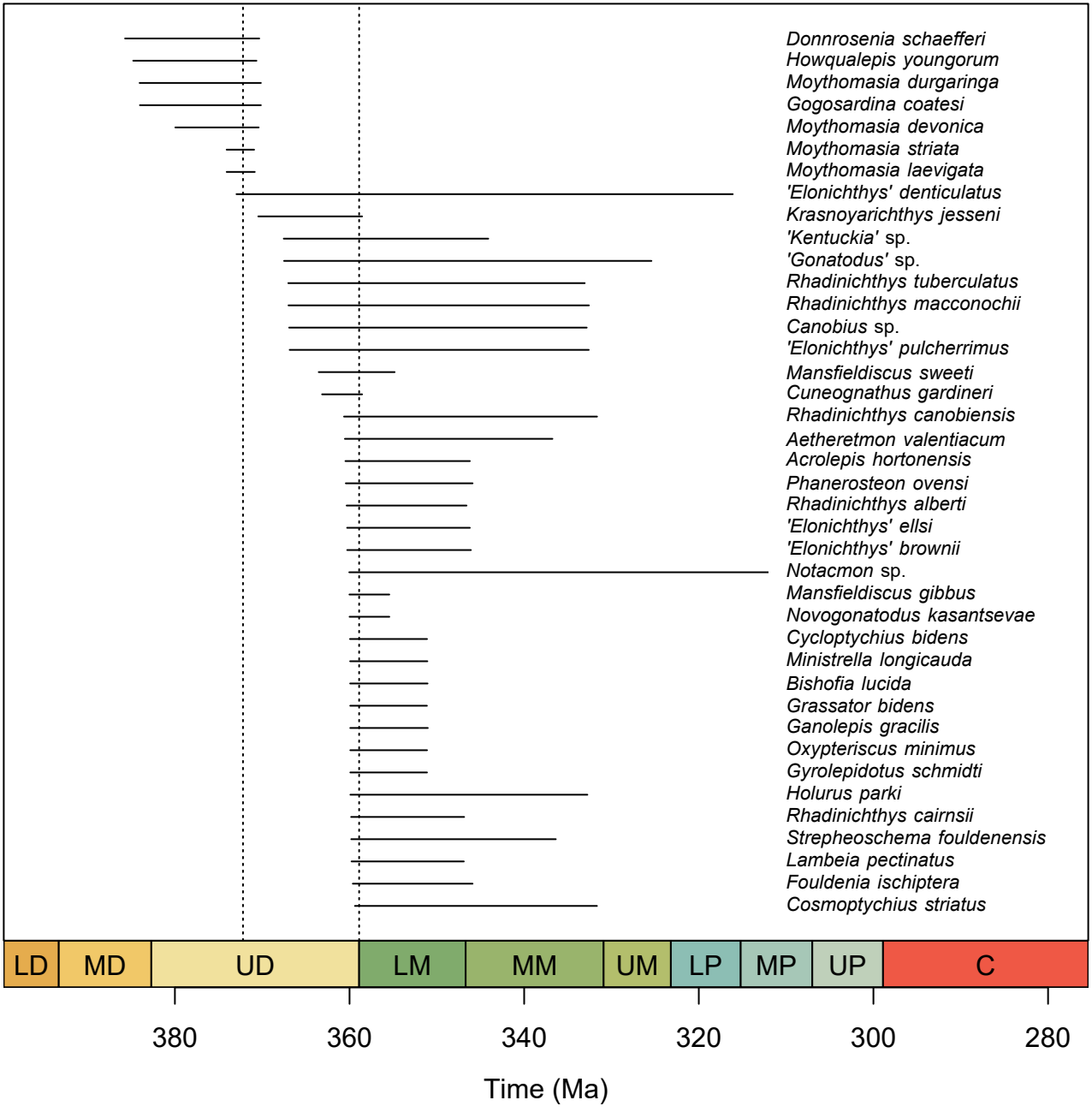
Donnrosenia schaefferi
Howqualepis youngorum
Moythomasia durgaringa
Gogosardina coatesi
Moythomasia devonica
Moythomasia striata
Moythomasia laevigata
'Elonichthys' denticulatus
Krasnoyarichthys jesseni
'Kentuckia' sp.
'Gonatodus' sp.
Rhadinichthys tuberculatus
Rhadinichthys macconochii
Canobius sp.
'Elonichthys' pulcherrimus
Mansfieldiscus sweeti
Cuneognathus gardineri
Rhadinichthys canobiensis
Aetheretmon valentiacum
Acrolepis hortonensis
Phanerosteon ovensi
Rhadinichthys alberti
'Elonichthys' ellsi
'Elonichthys' brownii
Notacmon sp.
Mansfieldiscus gibbus
Novogonatodus kasantsevae
Cycloptychius bidens
Ministrella longicauda
Bishofia lucida
Grassator bidens
Ganolepis gracilis
Oxypteriscus minimus
Gyrolepidotus schmidti
Holurus parki
Rhadinichthys cairnsii
Strepheoschema fouldenensis
Lambeia pectinatus
Fouldenia ischiptera
Cosmoptychius striatus
LD
MD
UD
LM
MM
UM
LP
MP
UP
C
380
360
340
320
300
280
Time (Ma)

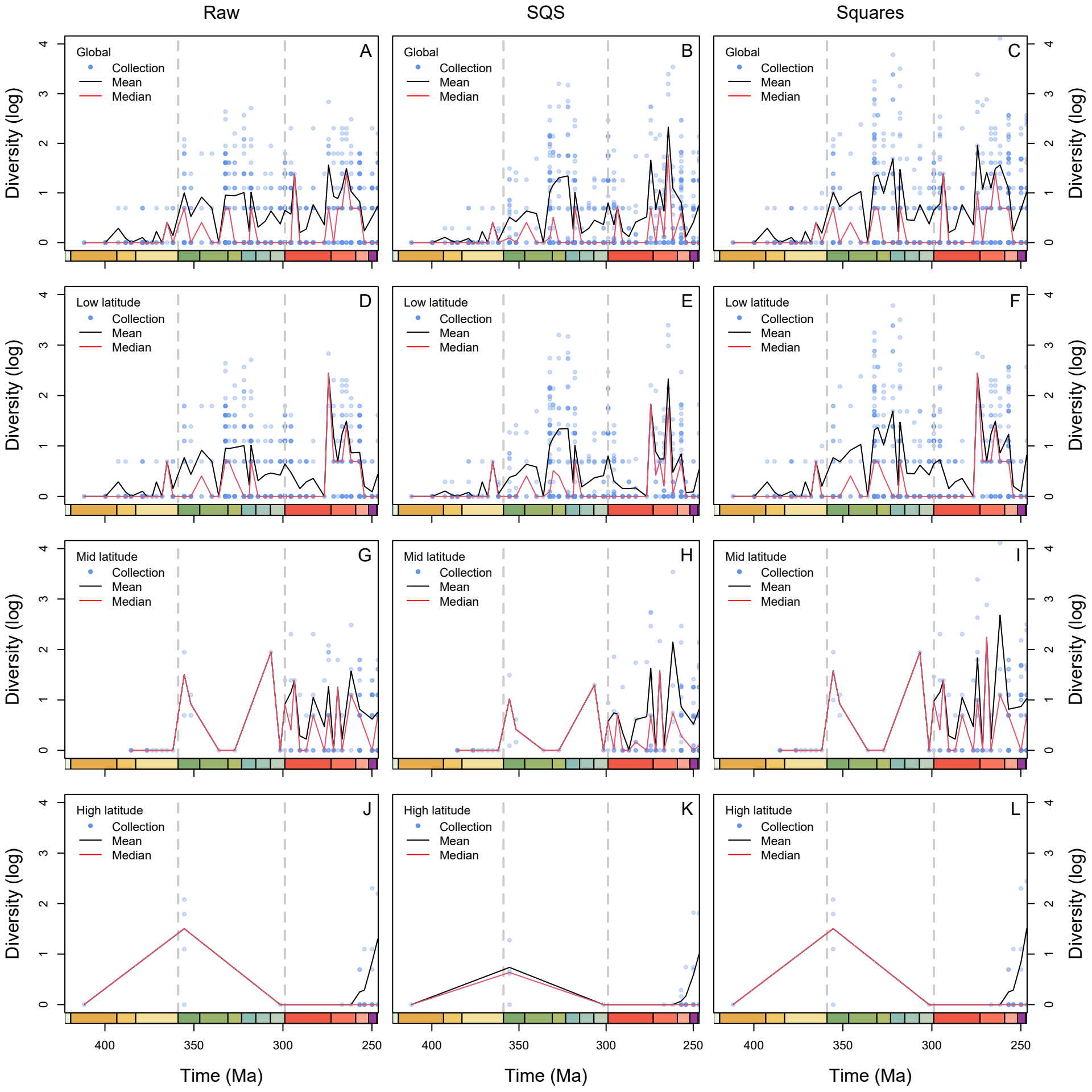
Raw
SQS
Squares
Global
Low latitude
Mid latitude
High latitude
Collection
Mean
Median
A
B
C
D
E
F
G
H
I
J
K
L
Diversity (log)
Time (Ma)
400
350
300
250